AD-758 158

A PRECISION YAWSONDE CALIBRATION TECHNIQUE

Wallace H. Clay

Ballistic Research Laboratories
Aberdeen Proving Ground, Maryland

January 1973

DISTRIBUTED BY:

NTIS

National Technical Information Service
U. S. DEPARTMENT OF COMMERCE
5285 Port Royal Road, Springfield Va. 22151

BRL MR 2263

BRL

AD

AD758158

MEMORANDUM REPORT NO. 2263

A PRECISION YAWSONDE CALIBRATION TECHNIQUE

by

Wallace H. Clay

January 1973

Approved for public release; distribution unlimited.

Reproduced by
NATIONAL TECHNICAL
INFORMATION SERVICE
U S Department of Commerce
Springfield VA 22151

D D C
RECEIVED
APR 5 1973
B

43

USA BALLISTIC RESEARCH LABORATORIES
ABERDEEN PROVING GROUND, MARYLAND

Destroy this report when it is no longer needed.
Do not return it to the originator.

Secondary distribution of this report by originating or sponsoring activity is prohibited.

Additional copies of this report may be purchased from the U.S. Department of Commerce, National Technical Information Service, Springfield, Virginia 22151

ACCESSION for

NTIS White Section ☑
DDC Buff Section ☐
UNANNOUNCED ☐
JUSTIFICATION .....

BY .....
DISTRIBUTION/AVAILABILITY CODES

Dist.	AVAIL. and/or SPECIAL	
A		

The findings in this report are not to be construed as an official Department of the Army position, unless so designated by other authorized documents.

UNCLASSIFIED

Security Classification

DOCUMENT CONTROL DATA - R & D

(Security classification of title, body of abstract and indexing annotation must be entered when the overall report is classified)

1. ORIGINATING ACTIVITY *(Corporate author)* U. S. Army Ballistic Research Laboratories Aberdeen Proving Ground, Maryland 21005	2a. REPORT SECURITY CLASSIFICATION Unclassified 2b. GROUP

3. REPORT TITLE

A PRECISION YAWSONDE CALIBRATION TECHNIQUE

4. DESCRIPTIVE NOTES *(Type of report and inclusive dates)*

5. AUTHOR(S) *(First name, middle initial, last name)*

WALLACE H. CLAY

6. REPORT DATE JANUARY 1973	7a. TOTAL NO. OF PAGES 52	7b. NO. OF REFS 3
8a. CONTRACT OR GRANT NO. b. PROJECT NO. RDT&E 1T061102A33D c. d.	9a. ORIGINATOR'S REPORT NUMBER(S) MEMORANDUM REPORT NO. 2263 9b. OTHER REPORT NO(S) *(Any other numbers that may be assigned this report)*	

10. DISTRIBUTION STATEMENT

Approved for public release; distribution unlimited.

11. SUPPLEMENTARY NOTES	12. SPONSORING MILITARY ACTIVITY U. S. Army Materiel Command Washington, D. C. 20315

13. ABSTRACT

A technique has been developed for the accurate calibration of yawsondes of the Harry Diamond Laboratory type to provide a calibration accurate to within .1 degree. The current system can be applied to calibration of yawsonde made at the Ballistic Research Laboratories with the same accuracy as the HDL type.

Details of illustrations in
this document may be better
studied on microfiche

I

DD FORM 1 NOV 65 1473 REPLACES DD FORM 1473, 1 JAN 64, WHICH IS OBSOLETE FOR ARMY USE.

UNCLASSIFIED

Security Classification

UNCLASSIFIED

Security Classification

14 KEY WORDS	LINK A ROLE	LINK A WT	LINK B ROLE	LINK B WT	LINK C ROLE	LINK C WT
Calibration						
Yawsonde						
Solar Aspect Angle						
Optical Alignment						
Sun Sensor						

II

UNCLASSIFIED

Security Classification

B A L L I S T I C R E S E A R C H L A B O R A T O R I E S

MEMORANDUM REPORT NO. 2263

JANUARY 1973

A PRECISION YAWSONDE CALIBRATION TECHNIQUE

Wallace H. Clay

Exterior Ballistics Laboratory

Approved for public release; distribution unlimited.

RDT&E Project No. 1T061102A33D

A B E R D E E N P R O V I N G G R O U N D, M A R Y L A N D

B A L L I S T I C R E S E A R C H L A B O R A T O R I E S

MEMORANDUM REPORT NO. 2263

WHClay/ds/mjm
Aberdeen Proving Ground, Md.
January 1973

A PRECISION YAWSONDE CALIBRATION TECHNIQUE

ABSTRACT

A technique has been developed to calibrate yawsondes of the Harry Diamond Laboratories type. The calibration is accurate to within 0.1 degree. The current system can be applied to yawsondes made at the Ballistic Research Laboratories to obtain calibrations of similar accuracy.

Preceding page blank

TABLE OF CONTENTS

		Page
	ABSTRACT	3
	LIST OF ILLUSTRATIONS	7
	LIST OF SYMBOLS	9
I.	INTRODUCTION	13
II.	DESCRIPTION OF YAWSONDES	13
	A. The BRL Yawsonde	14
	B. The Harry Diamond Laboratories Yawsonde	15
III.	YAWSONDE CALIBRATION	15
	A. General Requirements of a Calibration System	16
	B. Initial Calibration Systems	17
	C. Current Calibration System	19
	D. Results	21
	E. Future Calibrations	22
IV.	CONCLUSION	23
	REFERENCES	40
	APPENDIX A	41
	DISTRIBUTION LIST	47

Preceding page blank

LIST OF ILLUSTRATIONS

Figure		Page
1.	BRL Sun Sensor	26
2.	BRL Sun Sensor Orientation	27
3.	Sketch of Basic Principle of HDL Yawsonde	28
4.	HDL Yawsonde Mounted in Nose Fuse of an Artillery Shell	29
5.	Basic Geometry of HDL Yawsonde	30
6.	Initial Calibration Systems	31
7.	Original Calibration Fixture	32
8.	Schematic of Current Calibration System	33
9.	Current Calibration Fixture Showing Rotary Table and Indexed Dividing Head	34
10.	Typical Calibration Signals from HDL Yawsonde	35
11.	Schematic of Alignment Tool	36
12.	Optical Alignment Tool	37
13.	Sketch of the Optics for the Alignment of the Light Beam	38
14.	Typical Calibration Curve for HDL Yawsonde	39
A-1.	Geometry of HDL Yawsonde Used in Analysis	44
A-2.	Cross Section of HDL Yawsonde Showing Geometry for Calculation of Roll Intercept Angles	45

Preceding page blank

LIST OF SYMBOLS

ℓ	the distance from the pin-hole to the solar cell of the HDL yawsonde.
x,y,n	an orthogonal coordinate system used for the analysis of the HDL yawsonde
x_1	the distance from the vertex of the V formed on the solar cell to the origin of the coordinate system (for HDL yawsonde)
$\tilde{x}$	the identity: $\tilde{x} \equiv \sin(\Delta\phi/2)$
$\hat{s}$	the solar vector, extending from the sun to the center of gravity of the projectile
t	the period of time between successive signals from both sensors (BRL yawsonde) or from the upper and lower legs of the V (HDL yawsonde)
A,B	constants related to the geometry of the HDL yawsonde
T	the period of time between successive rotations of the same sensor (BRL) (or the same legs of the V for HDL yawsondes) through the light beams
α	an angle representing misalignment between the light beam and the longitudinal axis of the projectile
β	an orientation angle between two sun sensors (BRL), measured around the circumference of the projectile
γ	an orientation angle (BRL yawsonde), the angle which the slit of the sensor makes with respect to the longitudinal axis of the projectile
δ_o	the half-angle of the V masked on the solar cell for the HDL yawsonde
η	the ratio of the refractive index of epoxy to the refractive index for air (HDL yawsonde)
σ	solar aspect angle, the angle between the longitudinal axis of the projectile and the solar vector $\hat{s}$
σ_n	the complement of the solar aspect angle
ϕ	roll angle, measured in a plane perpendicular to the longitudinal axis of the projectile
$\Delta\phi$	roll angle interval, the angle between successive roll orientations at which the light beam first appears within the field of view of each sun sensor

Preceding page blank

LIST OF SYMBOLS

Subscripts

i	refers to angles within the epoxy of the HDL yawsonde
u,L	refers to upper and lower legs of the V (HDL yawsonde)
1,2	refers to the two roll angles at which the amplitude of the voltage signals are maximum in the calibration of yawsondes.

Preceding page blank

I. INTRODUCTION

The dynamic motion of a projectile can be observed and measured over long flight paths using yawsondes.[1*] This is made possible by instrumenting the projectile with a high-g telemetry system. The pitching, yawing and rolling behavior is measured by sensors coupled to an active electronics payload on board the projectile. Solar aspect angle data are transmitted from the projectile to ground stations using an FM/FM telemetry system.[1]

The yawsonde is an instrument which measures solar aspect angle during the flight of the projectile. The solar aspect angle is the angle between the longitudinal axis of the projectile and a vector directed from the projectile to the sun. This angle is measured using light-sensitive silicon cells (or solar cells) which are mounted in fixtures that provide narrow fields of view in two planes. Voltage signals from the solar cells are amplified and made to modulate an oscillator whose output is transmitted from the projectile to a ground station. The geometrical arrangement of the solar cells is such that the phase relationships of the output pulses are a function of the solar aspect angle. Solar aspect angle data can be reduced to provide aerodynamic coefficients for a given projectile.

This report describes the yawsondes currently in use with a short analysis of their operation. The body of this report describes methods used to obtain a precise, physical calibration. The methods and accuracy of calibration are discussed.

II. DESCRIPTION OF YAWSONDES

Yawsondes of two different designs are used in projectiles at BRL. The two types of yawsondes operate on similar principles but differ in construction and in their optical fields of view.

*References are listed on page 40

Preceding page blank

A. The BRL Yawsonde

Figure 1 shows a BRL solar aspect sensor which consists of a silicon photovoltaic cell encapsulated in a plastic disk. A 4 degree by 150 degree field of view is established using a slot formed by two plates of black-anodized aluminum. The plates are serrated to prevent internal reflections and are so assembled to give an acceptance angle of 4 degrees. The end pieces of the slot are stainless steel with highly polished surfaces and arranged to give an acceptance angle of 150 degrees.

A yawsonde consists of two solar sensors mounted on a projectile so that each slot is at an angle γ with respect to the longitudinal axis of the projectile. The two sensing units are installed around the circumference of a projectile at an angular separation 2β. Figures 2-A and 2-B show the mounting of the sensors on a projectile.

As the projectile rotates about its longitudinal axis, light rays from the sun first appear in the field of view of one sensor and then in the field of view of the second sensor. Each time a sensor is exposed to the sun a voltage output results. The time between successive pulses from the same sensor is the roll period of the projectile. (The projectile is assumed not to yaw significantly during this period.) The time between successive pulses from different sensors is related to the solar aspect angle and thereby to the angle of attack of the projectile.

If the two sensors are oriented symmetrically on the projectile (i.e., if the magnitude of the angle γ is the same for each) the following relationship can be shown:[1]

$$\tan \sigma = \frac{\tan \gamma}{\sin (\Delta\phi/2 - \beta)} \tag{1}$$

where σ is the solar aspect angle and $\Delta\phi$ is the roll angle of the projectile between successive pulses from different sensors.

B. The Harry Diamond Laboratories Yawsonde

The second type of yawsonde used by the BRL is a pin-hole sensor developed at the Harry Diamond Laboratories (HDL).[2] Figure 3 shows a sketch of the HDL sonde and Figure 4 shows the sonde mounted in a nose fuze configuration for an artillery projectile.

The HDL yawsonde is made from a solid piece of moulded, transparent epoxy. The front and rear surfaces are copper-plated to block light. The field of view is defined by a pin-hole etched in the copper on the front surface and a V etched in the copper on the back surface. Light rays coincident with pin-hole and V strike a silicon solar cell on the back surface which produces a signal voltage.

The HDL yawsonde is designed so that the projectile longitudinal axis is in the plane of the solar cell and passes through the vertex of the V. The V is oriented with the vertex towards the nose of the projectile. The geometry of the pin-hole and V are shown in Figure 5. A light ray, $\hat{s}$, enters the pin-hole on the front surface and is refracted by the epoxy filler before striking the rear surface. The spin of the projectile about axis xx' allows the ray to successively cross the two legs of the V. The result is a series of pulses from the solar cell whose phase relationships are determined by both the spin rate of the projectile and the instantaneous angle σ_n between the normal to the projectile axis and the light ray $\hat{s}$. It is shown in Appendix A that σ_n is related to $\Delta\phi$ by the equation

$$\tan\left[\sin^{-1}\left(\frac{1}{\eta}\sin\sigma_n\right)\right] = A \cdot \tan\left[\sin^{-1}\left(\frac{1}{\eta}\sin\Delta\phi/2\right)\right] - B \qquad (2)$$

where η is the ratio of refraction index of epoxy to air, and A and B are constants related to the yawsonde geometry.

III. YAWSONDE CALIBRATION

Yawsondes must be calibrated prior to use. Since the geometry and physical dimensions of the BRL yawsonde are well known Equation (1) could be used to calibrate the yawsonde. A physical calibration should

also be performed to insure that the yawsondes are symmetrically installed at the correct angle γ. The HDL yawsondes, however, are assembled with the dimensions and angular settings known only nominally. Moreover, the refraction index of the epoxy between pin-hole and solar cell is not well known. Therefore, the HDL yawsonde must be physically calibrated.

A. General Requirements of a Calibration System

A calibration system for yawsondes must meet the following general requirements:

1. Flight Simulation. The motion of the projectile in flight must be simulated in the laboratory. A device to rotate the projectile or yawsonde must be provided as well as a means of simulating yawing motion of the projectile.

2. Light Source. The calibration system must have a light source which simulates the parallel light of the sun. This source must have enough intensity to provide a reasonable signal for the solar cells. The diameter of the collimated light beam must be large enough to include the sensors as the projectile is yawed and rotated about its axis; the beam should be at least as wide as the diameter of the projectile at the location of the sensors.

3. Alignment. The light-source/optics combination alignment to the longitudinal axis of the shell must be well known. This requirement establishes a reference for the pitch or yaw angle. A method of measuring the light-source/optics alignment is needed.

4. Measurement of Roll and Yaw Angles. The roll and yaw angles of the projectile must be measured during the calibration. The resolution required of the measurement system depends upon the accuracy needed for the calibrations.

5. Accuracy. The accuracy of the calibration is determined by the specific apparatus and technique developed. For the yawsonde calibrations that are described in this report, the requirement was an accuracy of 0.2 degree in yaw; if the roll angle is known, then the calibration should give the yaw angle to within 0.2 degree.

B. Initial Calibration Systems

A schematic of the initial calibration system is shown in Figure 6. A carbon arc was used as a high intensity light source. A seven-inch focal length lens, f (2.5), collimated the light from the carbon arc. The projectile with yawsonde was mounted in a fixture that allowed the projectile to be rotated about its longitudinal axis and also about an axis perpendicular to the plane containing light beam and the longitudinal axis of the projectile. Thus, the yawing and rolling motion of the projectile could be simulated. In an earlier version of the calibrator, rolling motion was obtained by spinning the projectile about its longitudinal axis with an electric motor and pulley arrangement (Figures 6a. and 7). The missile was yawed by hand. The light beam was aligned to be normal to the projectile using a fixture which slips over the projectile at the position of the yawsonde. This fixture had a highly polished surface parallel to the projectile's axis. Alignment consisted of reflecting the light beam back upon itself so that the position of zero yaw could be determined to within ± 0.5 degree.

The calibration procedure consisted of the following steps. The telemeter electronics were turned on. The projectile was manually positioned to an angle of yaw and rotated using the motor-pulley arrangement. Radio frequency transmission was monitored with an FM receiver. The video signal was demodulated using a discriminator tuned to the center frequency of the telemeter voltage-controlled oscillator (VCO) and the data pulses were recorded on tape. This procedure was repeated for a range of yaw (usually from -40 to +40 degrees). After the calibration was complete the data on the tape were played back into an oscillograph recorder for calibration reduction. A typical set of data pulses is shown in Figure 6 (c).

Let us define T as the period between successive rotations of the same sensor through the light beam and t as the period between successive signals from both sensors. The roll angle between sensor intercepts

(at a given yaw angle) is then

$$\Delta\phi_{roll} = 2\pi \cdot \frac{t}{T} \tag{3}$$

and can be related to the solar aspect angle, σ, by (1) for the BRL yawsonde.

A different method of calibration is shown schematically in Figure 6 (b). A chopper was inserted in the beam between source and calibrator. The motor was removed from the fixture and the projectile rotated by hand. The solar cell outputs were displayed on an oscilloscope. The calibration procedure for this modified method was similar to the original method. The light source and optics were aligned so that the beam was perpendicular to the axis of the projectile. The projectile was then yawed at some angle σ. The projectile was rotated about its axis until one sun sensor intersected the light beam. The signal from the sensor was transmitted and displayed on the oscilloscope. The projectile roll orientation was adjusted until the displayed signal was a maximum. The orientation angle for maximum signal was measured on a scale fastened to the calibrator. The projectile was further rotated about its longitudinal axis until the signal from the second sensor was a maximum. The second roll angle was recorded and $\Delta\phi$, the difference in roll angle was determined. This process was repeated for as many angles as needed in the calibration.

The resolution in yaw and roll with this procedure was about 15 minutes of arc. The cumulative error was about 0.5 degree. The repeatability of calibration for either method above was about one degree. There are several reasons for the size of the errors and the lack of repeatability. In the original system the projectile was rotated about its axis by a motor-driven chain and the yawsonde pulses were eventually displayed on an oscillograph. The roll angle was measured by the time interval between pulses (see Figure 6 (c)). Variations in motor speed during one revolution would occur and lead to sizeable errors. Variations in tape recorder and oscillograph paper speed also contributed to the lack of repeatability between calibrations. For these reasons, a modified calibration technique was developed.

In the modified technique, the chopped output of the yawsonde is displayed directly on an oscilloscope. A maximum signal is sought and the corresponding roll angle is read off a vernier dial mounted on the fixture. This modified method uses the amplitude of the signal while the original method measured the period between signal pulses. The accuracy of the modified technique depends on the quality of the yawsonde signal which in turn depends on the steadiness of the light source and the sensitivity of the signal handling equipment. At first the modified calibration system had poor repeatability, attributed to the carbon arc light source. The arc drive mechanism was erratic. Moreover the electrodes burn in a spiral fashion with a resultant wavering of light intensity which was quite apparent in the signal from the yawsonde. A precise determination of maximum amplitude was impossible.

C. Current Calibration System

The current calibration technique has been applied mainly to the calibration of HDL yawsondes. The general technique of calibration is the same for both HDL and BRL yawsondes and values given for accuracy apply to both.

The current method is similar to the modified method previously described (Figure 8) with the main difference being apparatus and equipment. The fixture which rotates and yaws the projectile is a precision, rotary table with a 3-jaw dividing head as shown in Figure 9. The rotary table sets the yaw angles of the projectile and has a calibrated dial with vernier capable of resolving 15 seconds of arc. The dividing head is mounted on the rotary table and rotates the projectile or yawsonde about its longitudinal axis. The yawsonde is attached to the dividing head so that the sensor is directly over the center of the rotary table. Thus the field of view of the sensor remains within the parallel light beam for all yaw angles. The resolution of the graduated scale with vernier located on the dividing head is 2.5 minutes of arc.

The carbon arc of the original system was replaced by a 25 watt, zirconium arc, point light source to eliminate the fluctuations in light

intensity associated with the carbon arc. The zirconium arc is a d.c. source and the beam must be mechanically chopped to provide an a.c. signal for the sensors. The chopping frequency was selected to be 225 hz. The small size of the zirconium source has some disadvantages. The mean source diameter is .030 inch and the average brightness is 23,000 candles per square inch. The crater size of the carbon arc, on the other hand, is .1 inch and the intensity is 80,000 candles per square inch. With the same optical system, the average radiant power in the zirconium arc beam is 40 times smaller than in the carbon arc beam. As a result the yawsonde sensors work with low signal levels and system noise becomes important. Figure 10 shows an oscilloscope trace of the chopped yawsonde output. The signal is approximately a square wave. Substantial noise in the flat portions of the wave makes the maximizing process difficult.

The signal-to-noise ratio of the system was improved by using a voltage-controlled oscillator to condition the yawsonde output with a tunable discriminator to retrieve the data. The discriminator low-pass cut-off filter was set to allow only frequencies below 300 Hz. The discriminator output is amplified and filtered through tunable band-pass filter. The band-pass filter output is monitored both on an oscilloscope and on a null voltmeter. The result of filtering is a stable and clear signal as shown in the bottom of Figure 10. The calibration procedure is the same as for the modified technique described earlier except that the maximum signal is now determined by a null meter.

The light beam and yawsonde are aligned by a different method than described earlier. A precise alignment tool, shown schematically in Figure 11, has been designed and consists of two perpendicular channels in a block of aluminum. A silvered mirror at the intersection of the two channels reflects the light 90 degrees. The axis xx' of the tool is colinear with the axis of the yawsonde. A detailed analysis of the alignment tool is given in reference 3.

The alignment procedure is quite simple. With the tool in the yawsonde fixture, light enters one channel, is reflected by the mirror, and exits the tool from the second channel. If the light beam is perpendicular

to the axis of the tool then light is reflected by the mirror only and a single image of the slit is observed on a screen placed at the exit. If the axis of the tool is slightly off the perpendicular to the light beam, then reflections of the light from the walls of the channel produce additional images of the slit at the exit. The system is aligned by rotating the table until a single image is observed at the exit. A photograph of the alignment tool is shown in Figure 12.

A sketch of the alignment optics is shown in Figure 13. Two external mirrors have been added to increase the optical arm of the reflected beam by 40 feet with a corresponding increase in alignment sensitivity to 4 minutes of arc per inch deflection. That is, a rotation of the fixture holding the alignment tool through 4 minutes of arc will cause the image of the slit to deflect a linear distance of one inch across the viewing screen. An operator error as great as 1/4 of an inch in adjusting the multiple images on the screen gives an alignment error of only one minute of arc.

D. Results

Some typical data from the calibration of an HDL yawsonde were obtained with the current calibration system and the method described in the previous section. Table I shows a set of calibration data for a single yawsonde. The angle σ_n, is preset. The angles ϕ_1 and ϕ_2 are the roll angles at which the sun sensor signal is a maximum. They are listed in degrees plus twelfths of degrees corresponding to the dial and vernier markings of the dividing head. Shown also in Table I is $\Delta\phi$. Table II shows the results of a repeatability test for the same yawsonde. The calibration was repeated ten times over a period of several days with different operators doing the calibrations. $\bar{\tilde{x}}$, for a given σ_n, is the quantity $\tilde{x} = \sin(\Delta\phi/2)$ averaged over the ten calibrations. The parameter $S_{d_{\tilde{x}}}$ is the standard deviation of the individual calibrations.

In the repeatability tests, σ_n was set to within 15 seconds of arc and $\Delta\phi$ was the measured quantity. In flight, however, $\Delta\phi$ (and hence $\tilde{x}$) is the measured quantity and σ_n is the unknown to be determined from

calibration. The accuracy in σ_n depends on the accuracy in $\Delta\phi$. If the uncertainty in $\tilde{x}$ is of the size of $S_{d_{\tilde{x}}}$, then the calibration data can be inverted and an uncertainty S_{d_σ}, in σ_n can be calculated. Values of S_{d_σ} are shown in Table II and are seen to be no greater than 0.1 degree. The repeatability tests were performed on other HDL yawsondes with similar results.

The geometrical and physical constants of the HDL yawsonde are known only nominally and a comparison of the calibration data with calculated values of σ_n cannot be made. Let us represent σ_n by a power series in $\sin(\Delta\phi/2)$.

$$\sigma_n = a_0 + a_1\tilde{x} + a_2\tilde{x}^2 + \ldots \tag{4}$$

where $\tilde{x} = \sin(\Delta\phi/2)$. The calibration data of Table I have been fitted by a fourth order polynomial in $\tilde{x}$. The data points and the fitted curve are compared in Figure 14 showing that a fourth order polynomial fits the data. The standard deviation of the fit is .07 degree. The data are smooth and can be readily repeated with accuracy. An error analysis of the calibration system, including alignment, resolution of the measuring equipment and the process itself shows that HDL yawsondes can be calibrated to within 0.1 degree.

E. Future Calibrations

There is a continuing need for calibration of HDL and BRL yawsondes. The system just described has until now been used only for HDL yawsondes but applies equally well to the BRL yawsonde. The apparatus must be changed slightly when BRL yawsondes are mounted in large projectiles such as 175mm and 155mm artillery shell. Different mounting fixtures will be needed to rotate the larger shells about their longitudinal axis. A 12-inch lens and a 100-watt zirconium arc lamp will be used with the larger projectiles. The basic method of calibration, however, will remain the same as described in this report.

IV. CONCLUSION

A technique has been developed to calibrate HDL and BRL yawsondes. The accuracy of the calibrator is better than 0.1 degree and the repeatability is within 0.1 degree. The system has been used to calibrate only HDL yawsondes but both system and method can be applied to the BRL yawsonde mounted in a variety of projectiles.

Table I. Typical Calibration Data

Angle of Yaw σ_n	Roll Angles ϕ_1	ϕ_2	Roll Interval $\Delta\phi = \phi_2 - \phi_1$
(degrees)	(degrees) + (1/12th's of a degree)		(degrees)
- 30	279/.25	302/3.75	23.29
- 25	276/5	304/10.5	28.46
- 20	274/0	307/5.75	33.48
- 15	271/7.75	310/.25	38.38
- 10	269/1	312/5.25	43.35
- 5	266/5.5	315/.5	48.58
0	263/8.25	317/8.75	54.04
+ 5	261/.25	320/7	59.56
+ 10	257/8.25	323/9.75	66.13
+ 15	254/.25	327/3.5	73.27
+ 20	250/2.25	331/1.75	80.96
+ 25	245/4	335/11.5	90.63
+ 30	239/9.5	341/5	101.63

Table II. Results of Repeatability Test

Yaw Angle σ_n	$\bar{\bar{x}} = \overline{\sin(\Delta\phi/2)}$	$S_{d_{\bar{\bar{x}}}}$	S_{d_σ}
(degrees)			(degrees)
- 30	.20271	.00065	.07
- 25	.24625	.00078	.10
- 20	.28731	.00048	.06
- 15	.32837	.00055	.07
- 10	.36976	.00044	.05
- 5	.41157	.00049	.06
0	.45431	.00027	.03
+ 5	.49868	.00048	.06
+ 10	.54576	.00066	.07
+ 15	.59604	.00077	.08
+ 20	.65052	.00069	.06
+ 25	.71047	.00059	.05
+ 30	.77548	.00097	.08

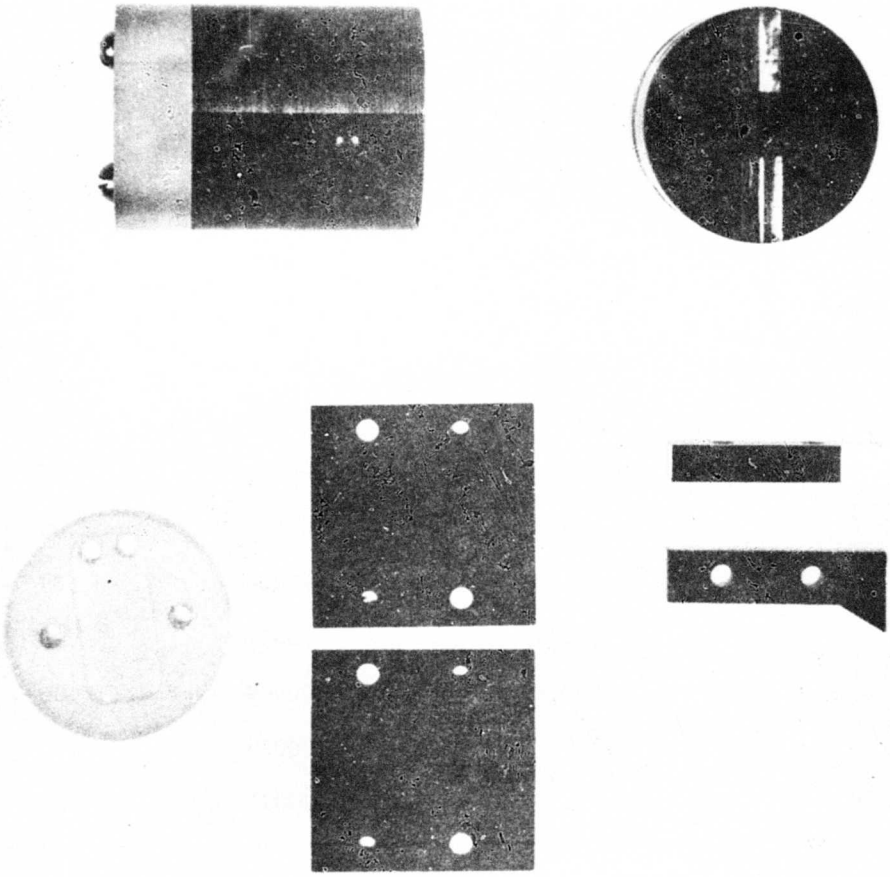

Figure 1. BRL Sun Sensor
Top: Side and Front View
Bottom: Assembly (Without Solar Cell)

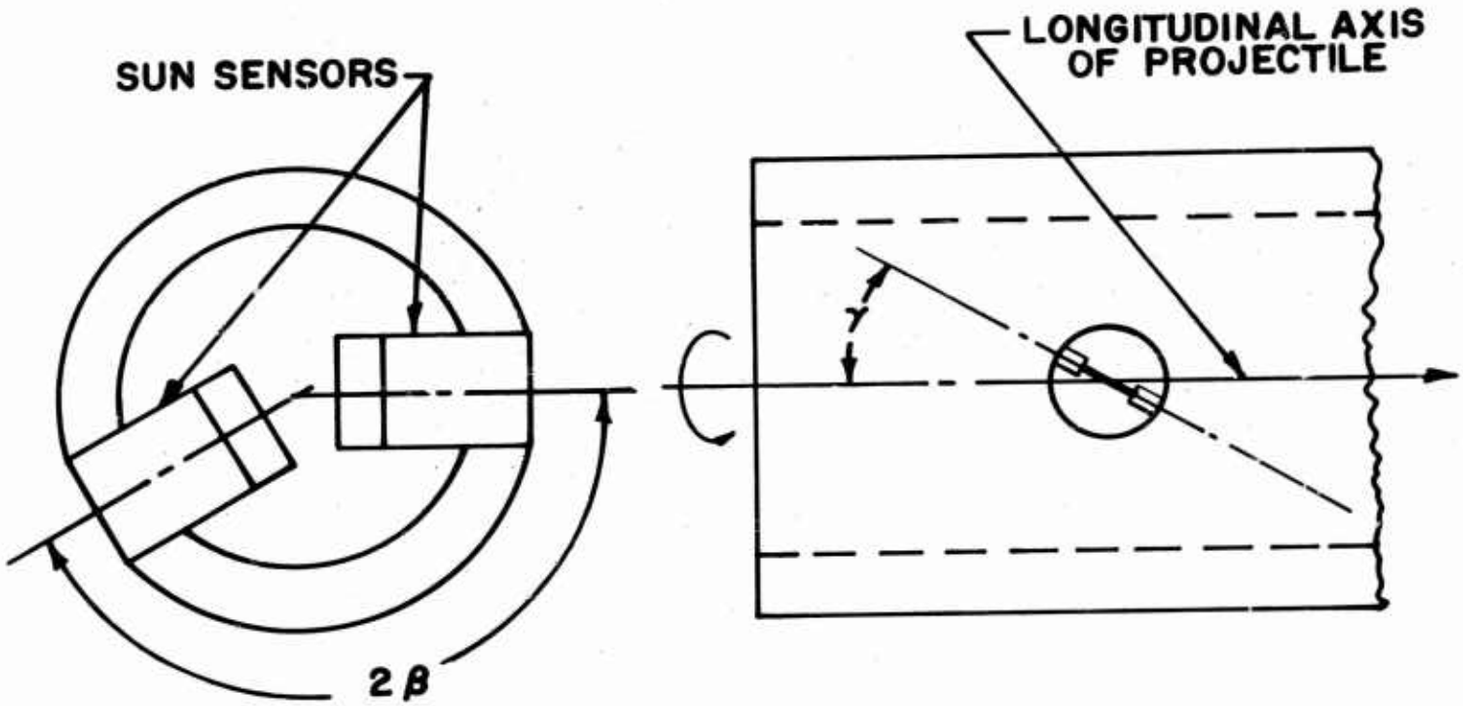

Figure 2. BRL Sun Sensor Orientation
Left: Orientation of Two Sensors Relative to Each Other
Right: Slit Inclination

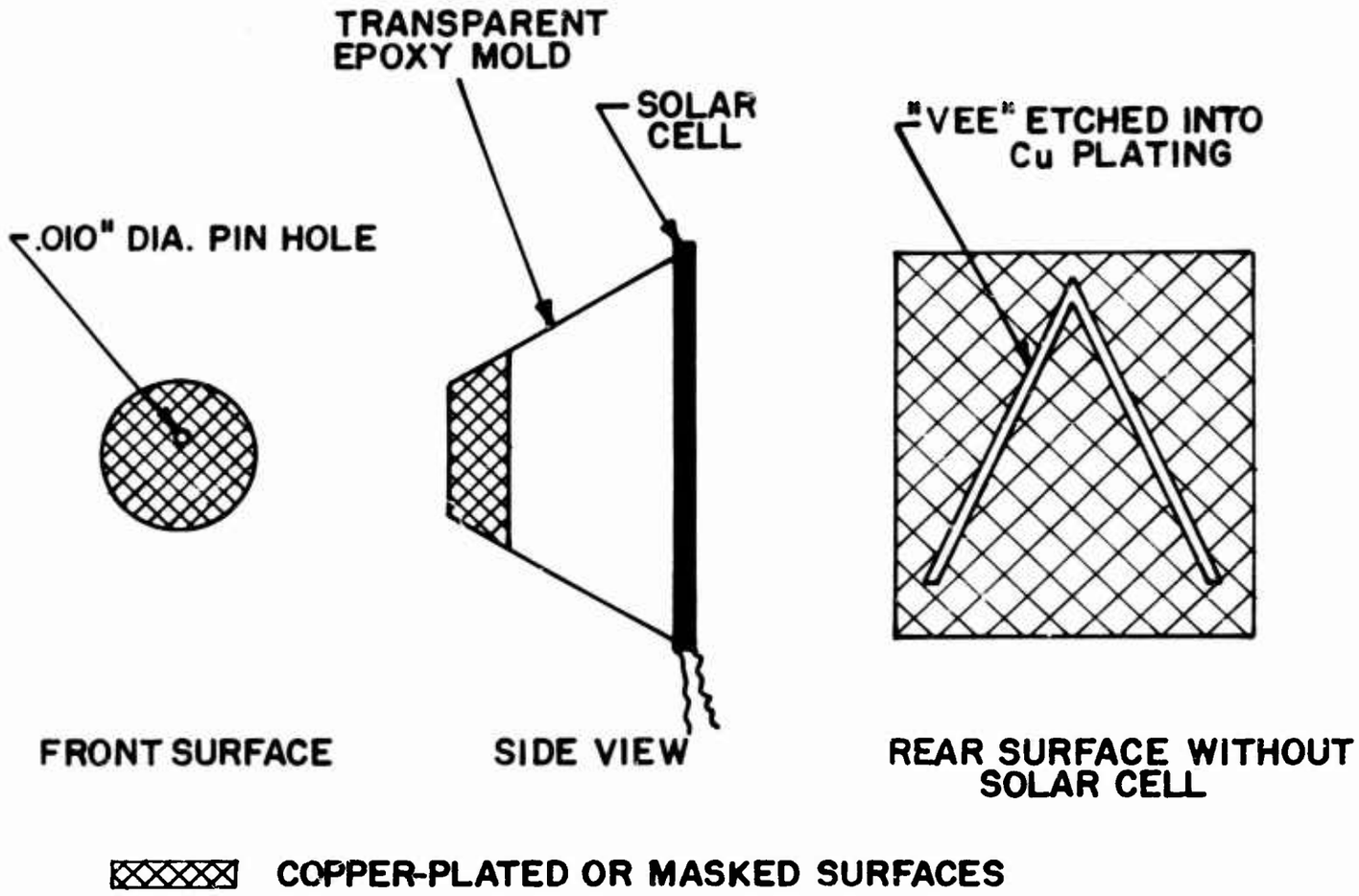

Figure 3. Sketch of Basic Principle of HDL Yawsonde

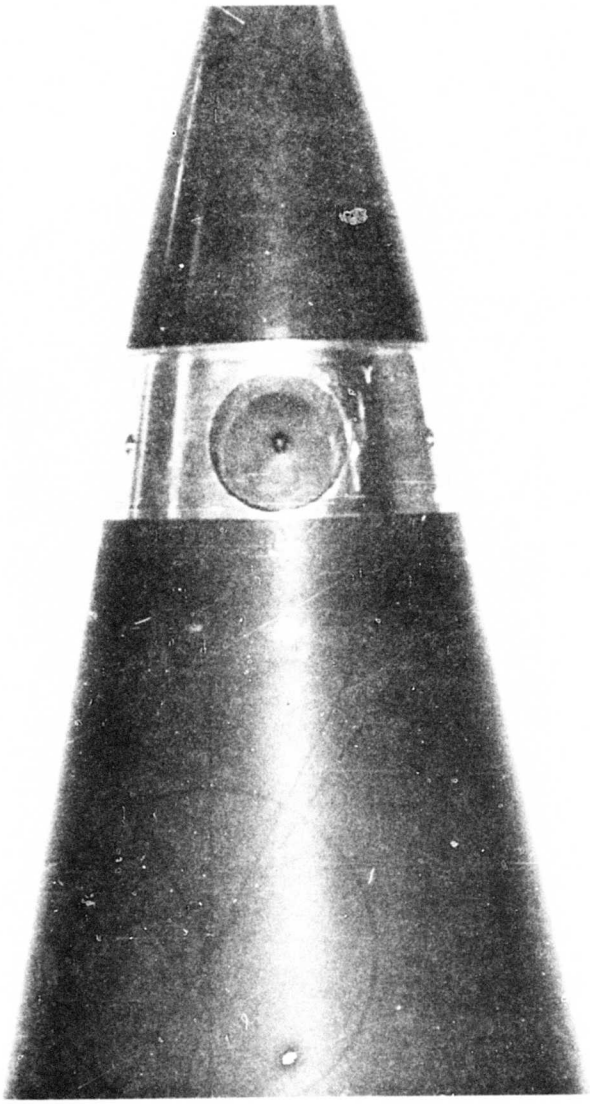

Figure 4. HDL Yawsonde Mounted in Nose Fuse of an Artillery Shell

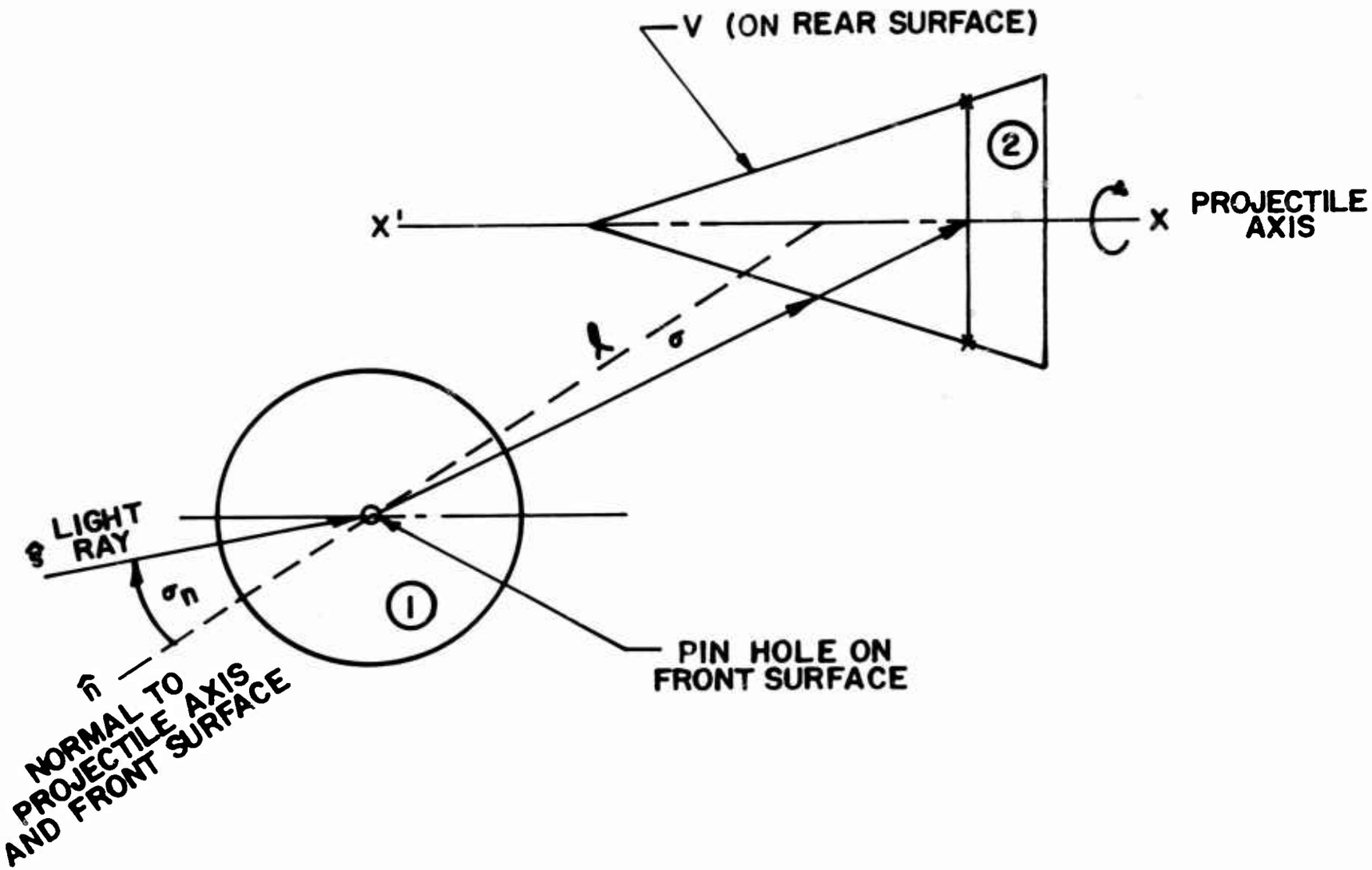

Figure 5. Basic Geometry of HDL Yawsonde

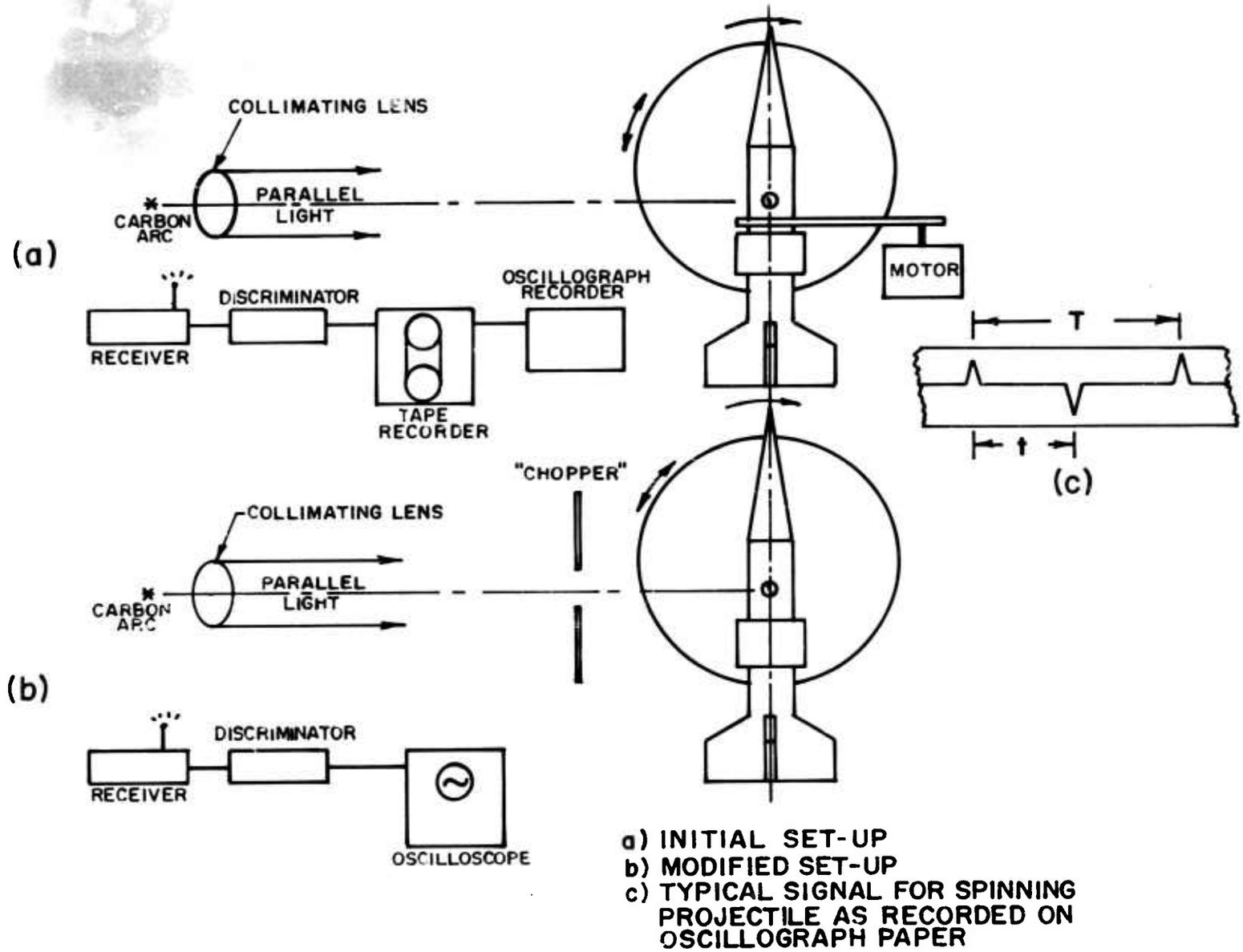

Figure 6. Initial Calibration Systems

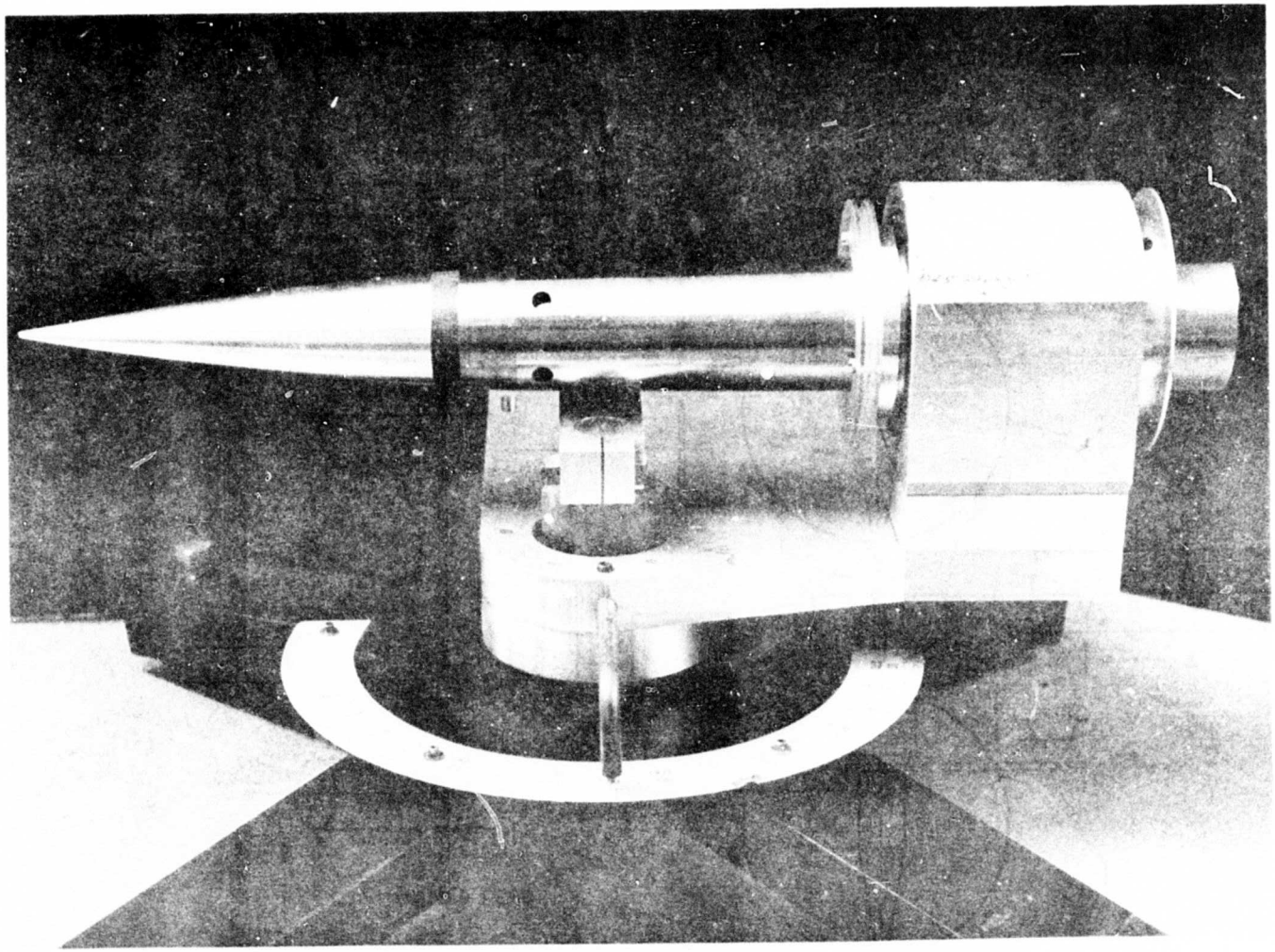

Figure 7. Original Calibration Fixture

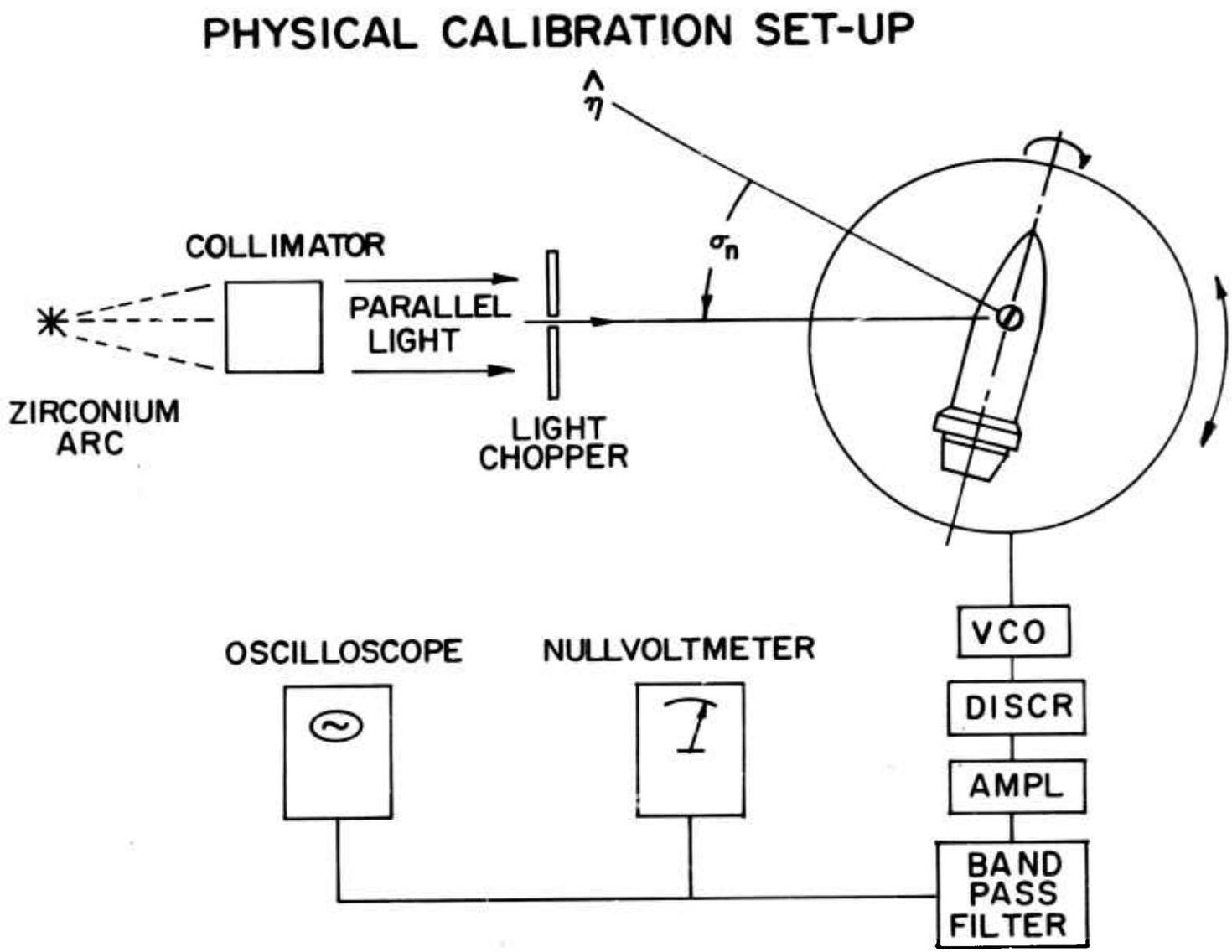

Figure 8. Schematic of Current Calibration System

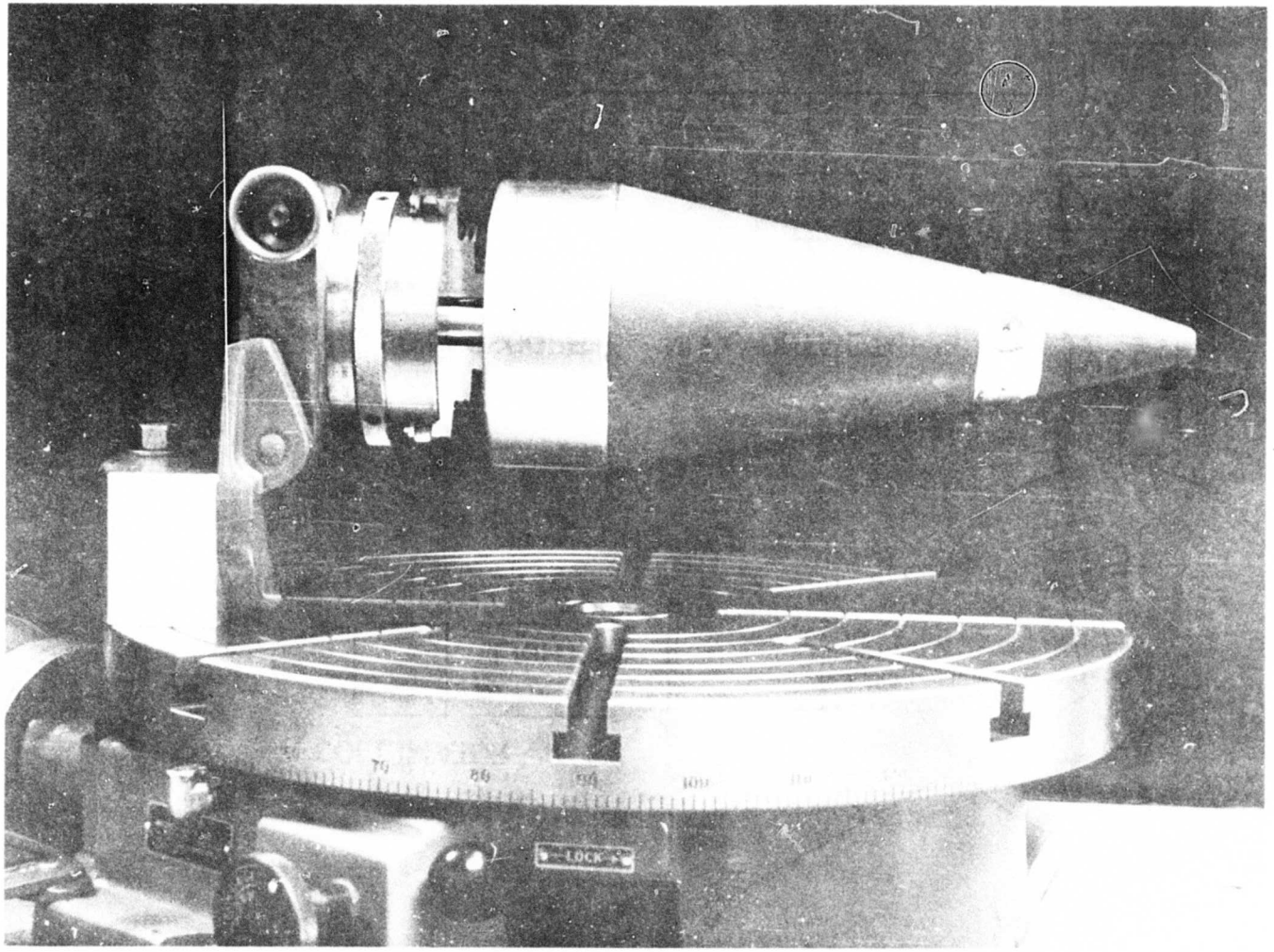

Figure 9. Current Calibration Fixture Showing Rotary Table and Indexed Dividing Head

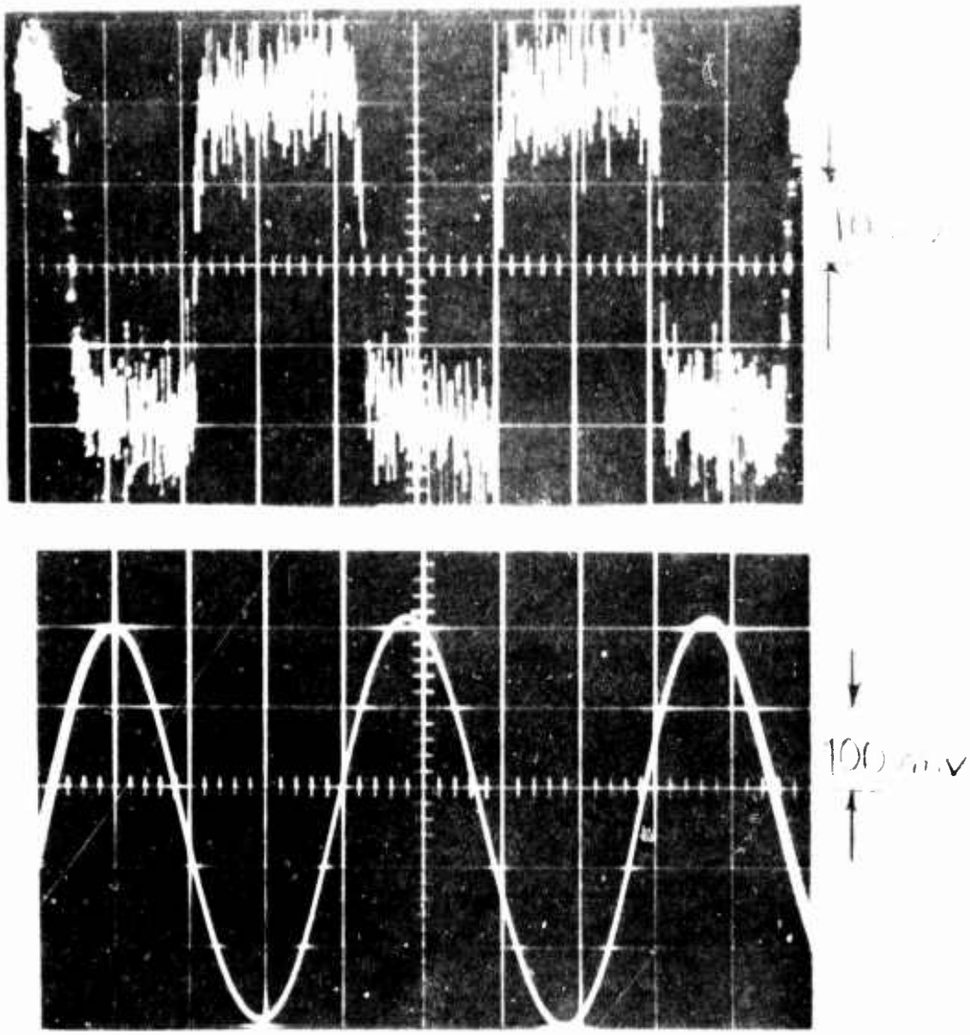

Figure 10. Typical Calibration Signal from an HDL Yawsonde
Top: Signal Output from Yawsonde in Response to Chopped Light Beam
Bottom: Conditioned Signal from Same Yawsonde

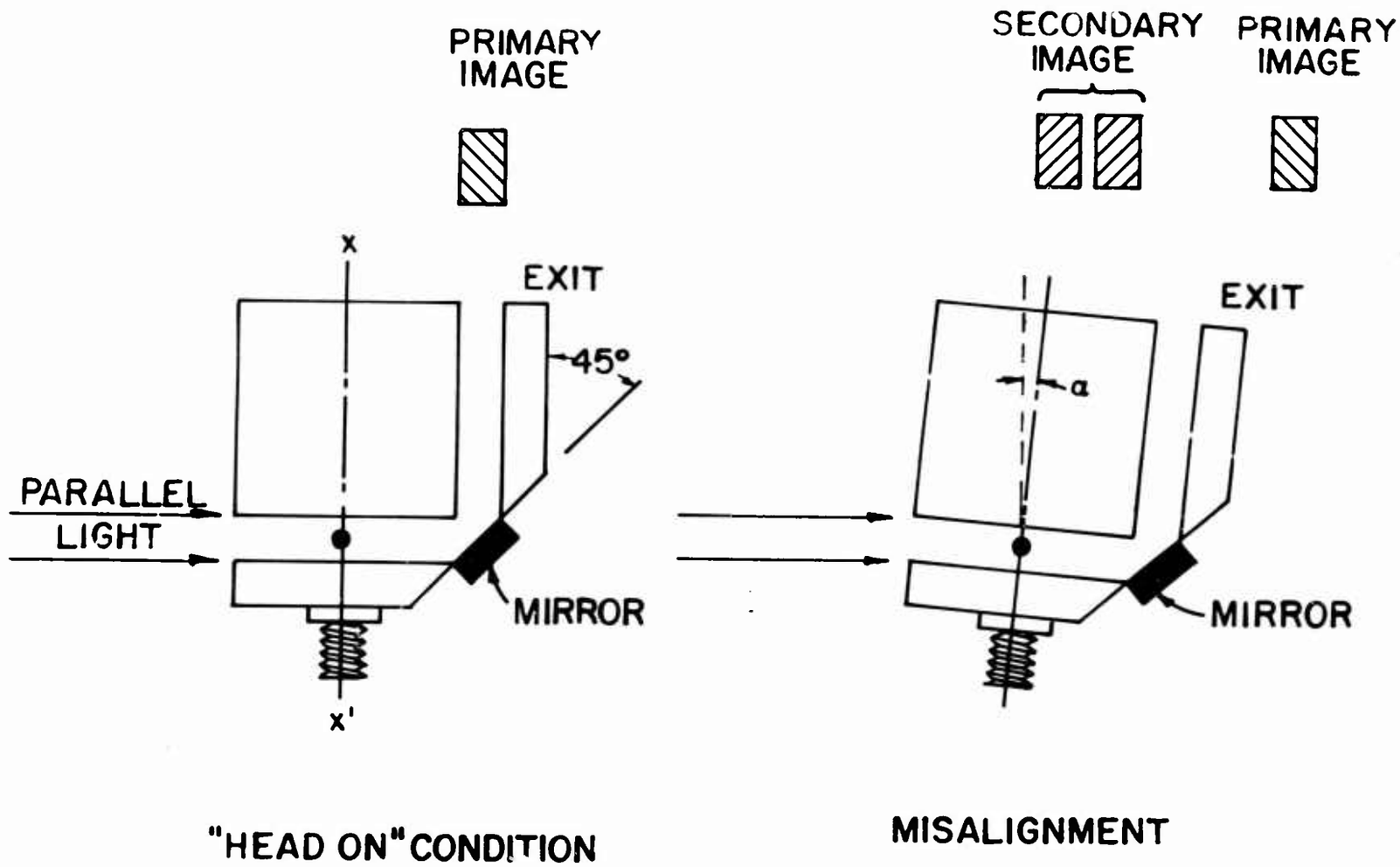

Figure 11. Schematic of Alignment Tool
Left: Light Beam Aligned Perpendicular to Axis xx'
Right: Light Beam Misaligned with Respect to Axis xx'

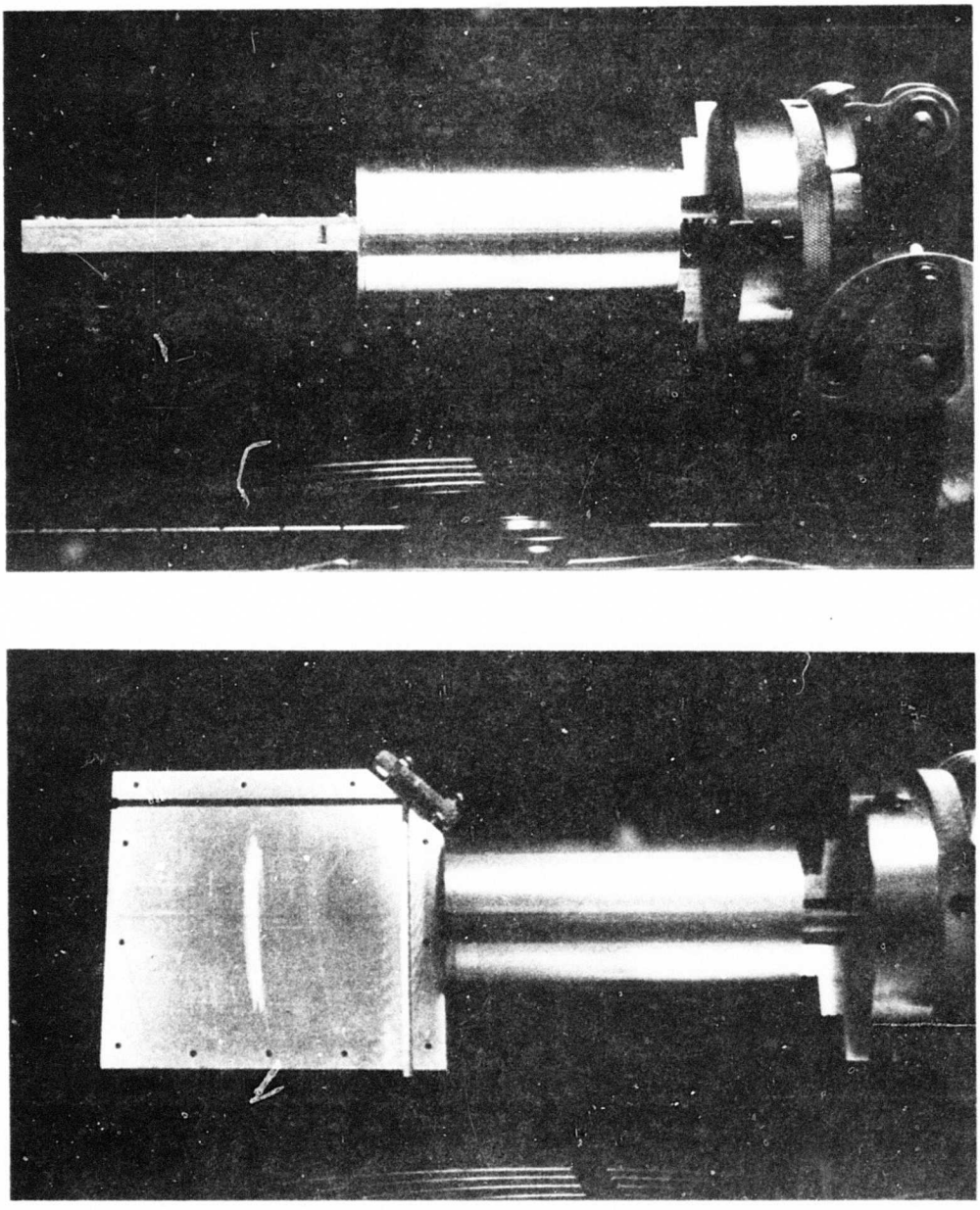

Figure 12. Photograph of Optical Alignment Tool
Top: Front View Showing Entrance Slit
Bottom: Top Plate Removed Showing Two Perpendicular Channels

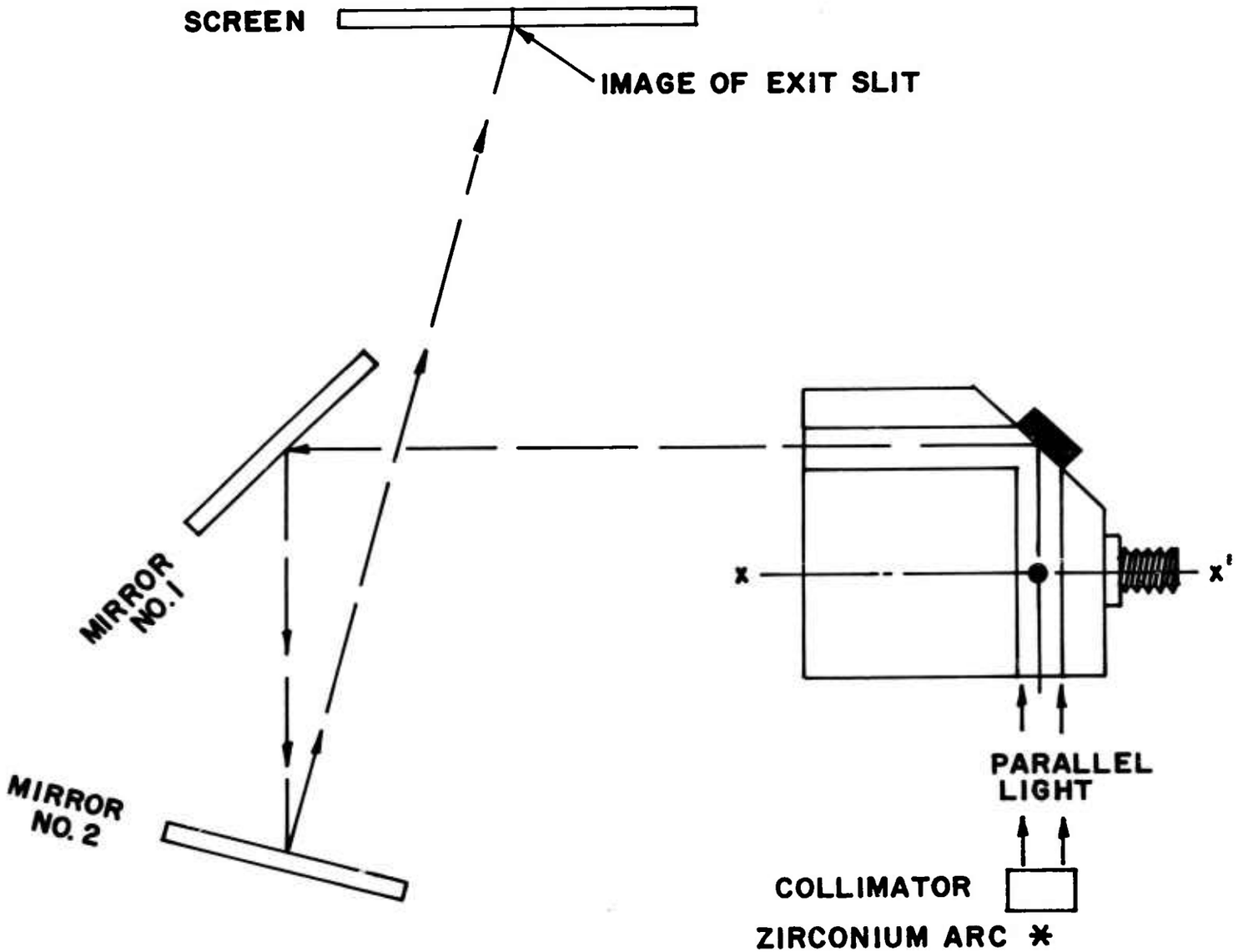

Figure 13. Sketch of the Optics for the Alignment of the Light Beam

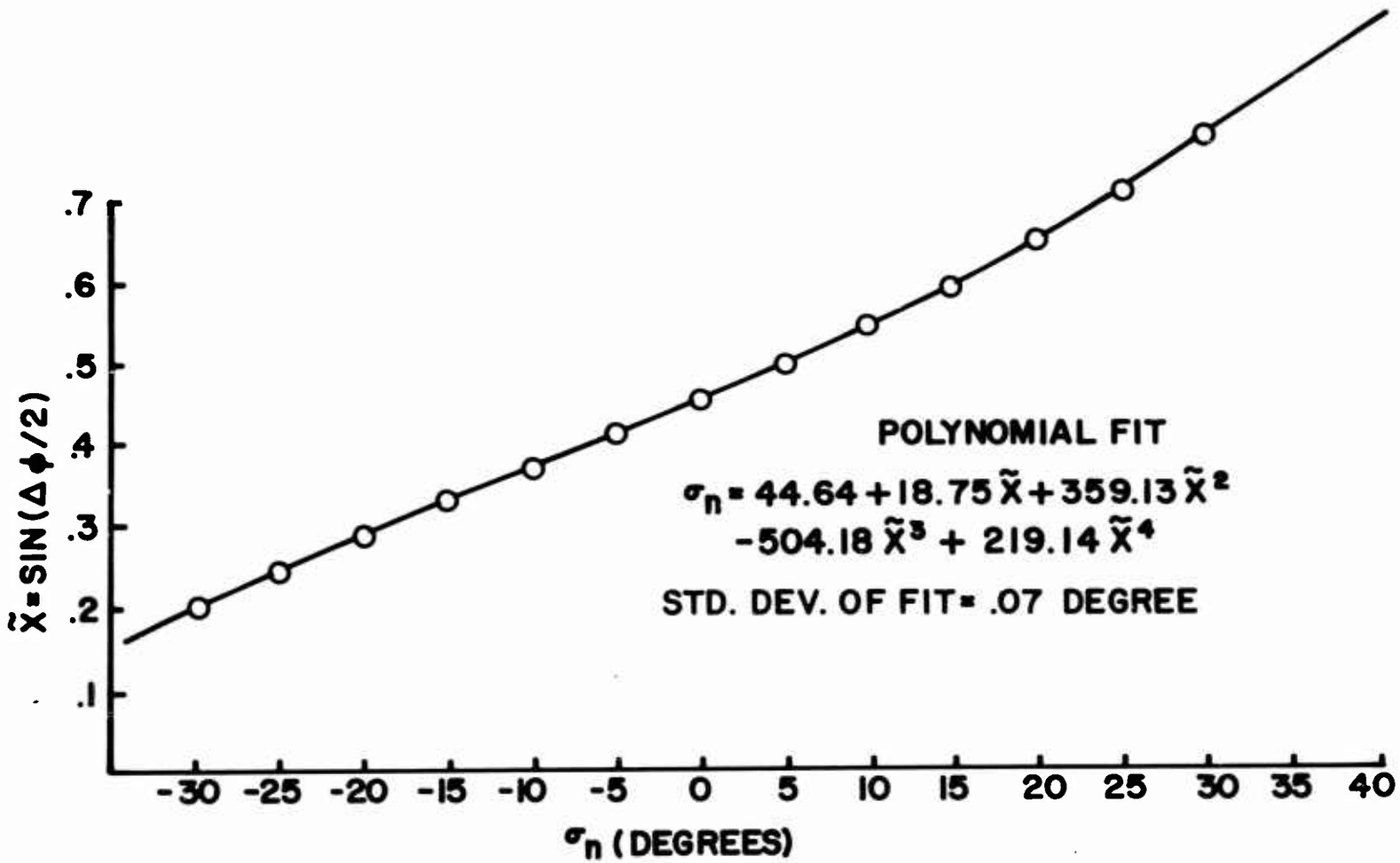

Figure 14. Typical Calibration Curve for HDL Yawsonde

REFERENCES

1. W. H. Mermagen, "Measurements of the Dynamical Behavior of Projectiles Over Long Flight Paths," *Journal of Spacecraft and Rockets*, Vol. 8, No. 4, April 1971, pp. 380-385; also published as Ballistic Research Laboratories Memorandum Report No. 2079, November 1970, AD 717002.

2. R. E. Elmore, "HDL Yawsonde Instrumentation," Harry Diamond Laboratory Report No. HDL-TM-71-19, September 1971.

3. W. H. Clay, "A Device and a Technique for Optically Aligning a Light Beam Relative to a Reference Axis," to be published as a Ballistic Research Laboratories Report.

APPENDIX A

Analysis of the HDL Pin-hole Yawsonde

The geometric arrangement of the pin-hole yawsonde is shown in Figure A-1. The silicon solar cell and the axis of symmetry, xx', of the projectile lie in the plane defined by the points A, B, and C. The lines $\overline{AB}$ and $\overline{AC}$ represent the unmasked V portion of the solar cell. Whenever light is incident on the V a voltage is generated by the solar cell. Consider a coordinate system consisting of three orthogonal axes x, y, and n. The x and y axes lie in the plane of the solar cell; n is perpendicular to this plane. The origin of the coordinate system at 0 is located so that the axis n passes through the pin-hole on the front surface of the sonde. The vector $\hat{s}$ represents the solar vector. The figure is drawn so that $\hat{s}$ lies in the plane containing the normal $\hat{n}$ and the axis of symmetry xx'.

Outside the yawsonde let $\hat{s}$ be at an angle σ_n with respect to the normal $\hat{n}$. The light ray is refracted between the pin-hole and the solar cell, finally arriving at point 1. The angle between the refracted ray and the normal $\hat{n}$ is denoted by σ_i. It is seen from the figure that as the projectile rolls about its axis xx', the refracted light ray intersects first one leg of the V and then the other leg (for example, at the points 2 and 3). Each intersection results in an electrical output from the cell. The angle through which the projectile rotates between intersections is called $\Delta\phi$.

The equations of the upper and lower legs of the V (Figure A-1) are

$$y_u = (\tan |\delta_o|) [x_1 + x]$$
$$y_L = -(\tan |\delta_o|) [x_1 + x] \qquad \text{(A-1)}$$

where δ_o is the half angle of the V and x_1 is the distance from the vertex of the V to the origin of the coordinate system. From Figure A-1

$$\tan \sigma_i = x/\ell \qquad \text{(A-2)}$$

where ℓ is the distance from the pin-hole to the solar cell.

Equation (A-1) can be rewritten, using Equation (A-2), as

$$y_u = \ell \, (\tan |\delta_o|) \, (x_1/\ell + \tan \sigma_i) \qquad \text{(A-3)}$$

$$y_L = -\ell \, (\tan |\delta_o|) \, (x_1/\ell + \tan \sigma_i)$$

The roll angle $\Delta\phi$ is related to y_u and y_L. Roll orientation of the projectile is measured in a plane which is perpendicular to the longitudinal axis of the projectile. Figures A-2(a), (b), (c) show the projection of the light-ray and the pin-hole of the sensor onto a plane which is perpendicular to the axis of rotation xx'. This plane is a crossection of the projectile that contains the points 1, 2, and 3 shown in Figure A-1. In Figure A-2(a), the roll orientation of the projectile is equivalent to that in Figure A-1. The refracted light beam strikes the solar cell at point (1). Figure A-2(b) shows the projectile rotated through an angle ϕ_u so that the refracted light ray strikes the solar cell at point (2) which is on the upper leg of the V. From the geometry of Figure A-2(b)

$$y_u = \ell \tan |\phi_{u_i}| \qquad \text{(A-4)}$$

where the subscript, i, indicates an internal angle. Figure A-2(c) shows the projectile rotated through an angle ϕ_L such that the light ray now strikes point (3) as indicated in the figure. From the figure

$$y_L = -\ell \tan |\phi_{L_i}| \qquad \text{(A-5)}$$

Combining Equations (A-3), (A-4), and (A-5),

$$|\phi_{u_i}| = \tan^{-1}[(\tan |\delta_o|)(x_1/\ell + \tan \sigma_i)] \qquad \text{(A-6)}$$

$$|\phi_{L_i}| = \tan^{-1}[(\tan |\delta_o|)(x_1/\ell + \tan \sigma_i)]$$

From (A-6) it is seen that $|\phi_{u_i}| = |\phi_{L_i}|$.

The internal angles ϕ_{u_i}, ϕ_{L_i} and σ_i are related to the external angles ϕ_u, ϕ_L and σ_n by Snell's Law:

$$\sin \sigma_n = \eta \sin \sigma_i \tag{A-7}$$

$$\sin \phi_u = \eta \sin \phi_{u_i}$$

$$\sin \phi_L = \eta \sin \phi_{L_i}$$

where η is the ratio of the index of refraction of epoxy to air.

Since $|\phi_{u_i}| = |\phi_{L_i}|$, then it is seen from Equation (A-7) that $|\phi_u|$ equals $|\phi_L|$.

The roll angle $\Delta\phi$ is defined by the equation

$$\Delta\phi = |\phi_u| + |\phi_L| \tag{A-8}$$

Therefore $|\phi_u| = |\phi_L| = \Delta\phi/2$ and Equations (A-7) and (A-6) can be combined to get the following equation relating $\Delta\phi$ and σ_n;

$$\begin{aligned} \sin^{-1}\left(\frac{1}{\eta} \sin (\Delta\phi/2)\right) &= |\phi_{u_i}| = |\phi_{L_i}| \\ &= \tan^{-1} \left[(\tan |\delta_o|)(x_1/\ell + \tan \sigma_i)\right] \\ &= \tan^{-1} \left[(\tan |\delta_o|)(x_1/\ell + \tan \{\sin^{-1}(\tfrac{1}{\eta} \sin \sigma_n)\})\right] \end{aligned} \tag{A-9}$$

Inverting Equation (A-9), we have

$$\tan \left[\sin^{-1}(\tfrac{1}{\eta} \sin \sigma_n)\right] = A \left(\tan \left[\sin^{-1}(\tfrac{1}{\eta} \sin \Delta\phi/2)\right]\right) - B \tag{A-10}$$

where $A = \cot |\delta_o|$ and $B \equiv x_1/\ell$. This is Equation (2) in Chapter II.

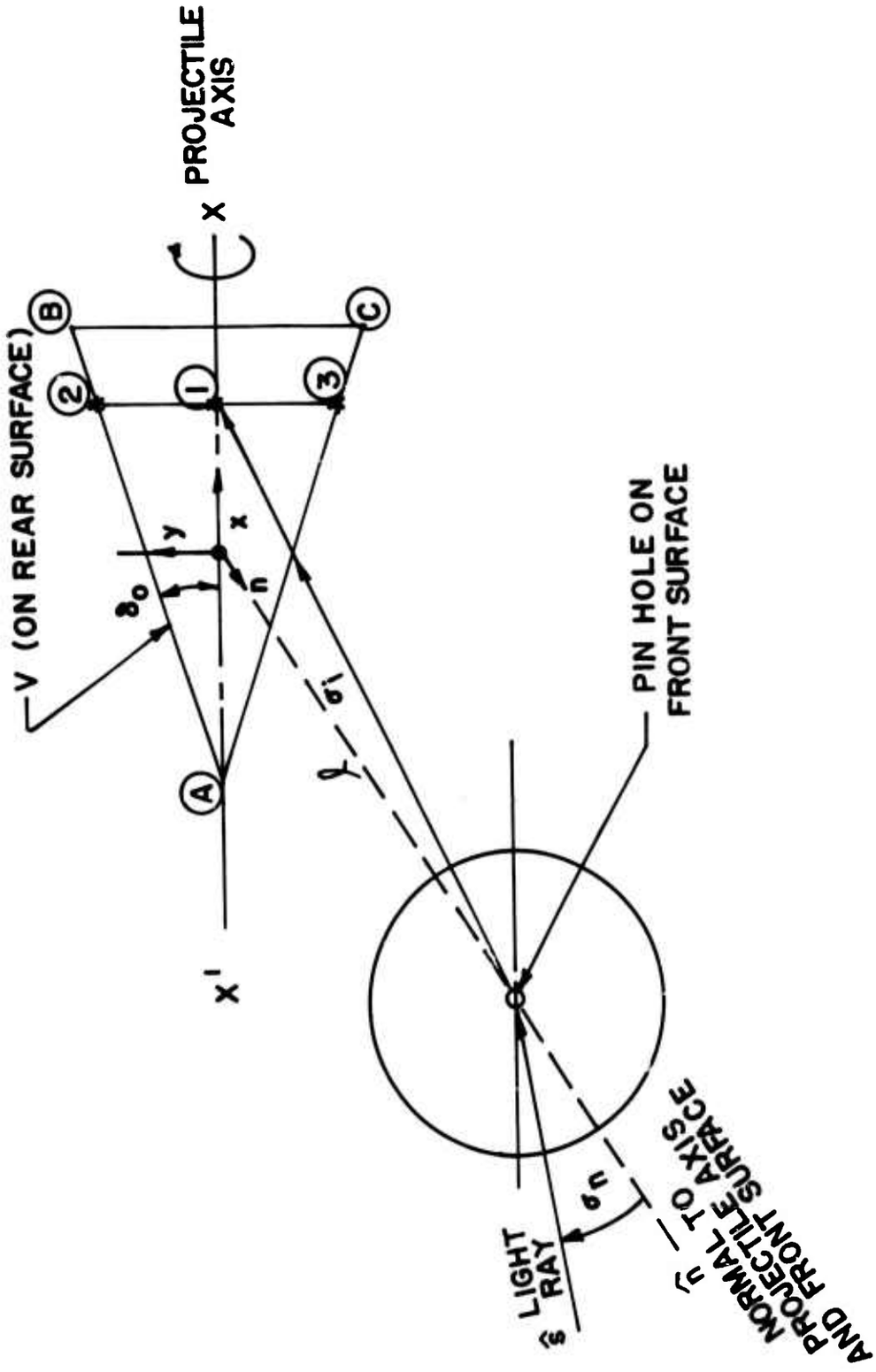

Figure A-1. Geometry for HDL Yawsonde Used in Analysis

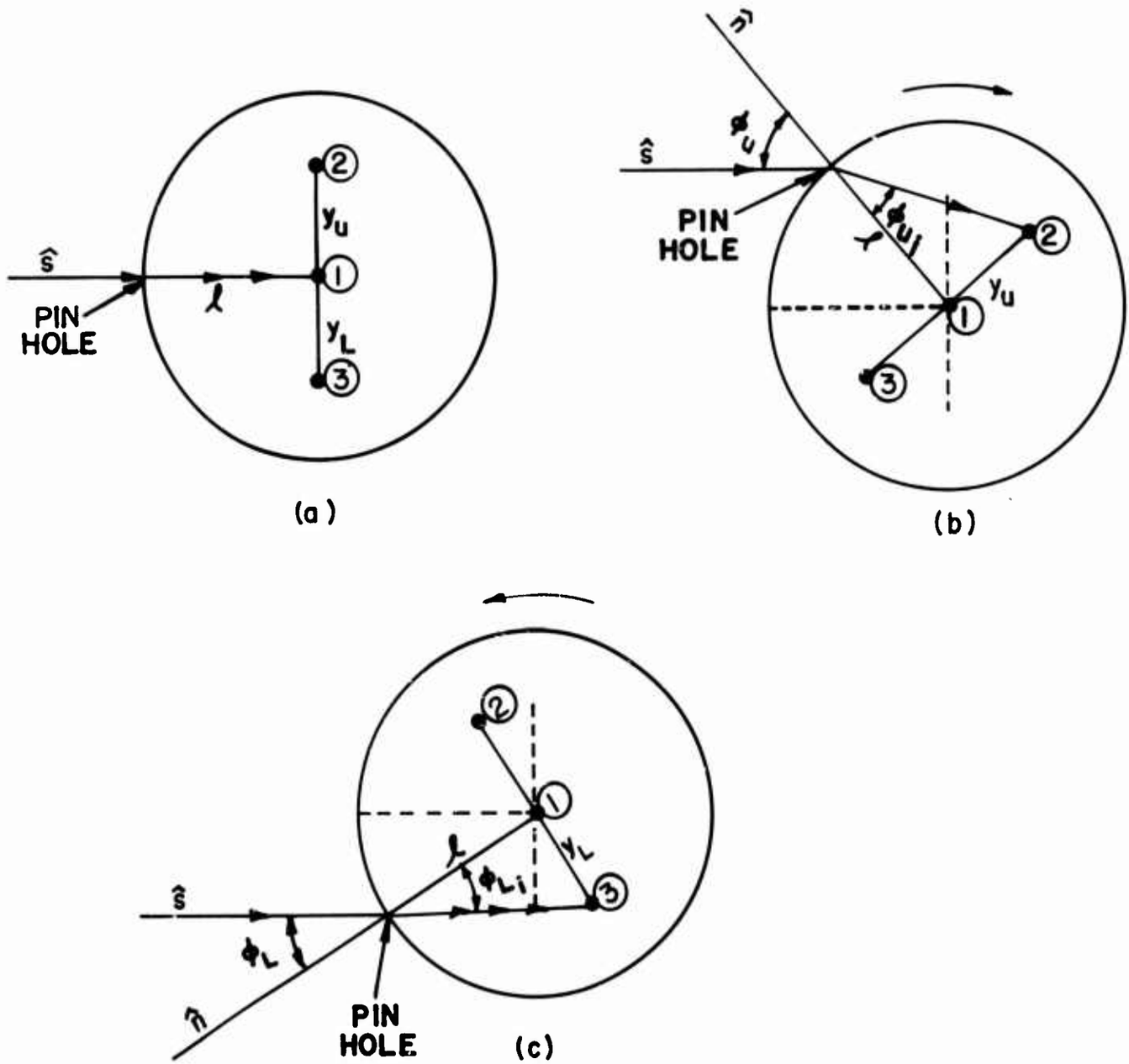

Figure A-2. Cross-Sectional Views of HDL Yawsonde Showing Geometry for the Calculation of Roll Intercept Angles